

**Two-Photon Excited Fluorescence of BF₂ Complexes of Curcumin
Analogues: Toward NIR-to-NIR Fluorescent Organic Nanoparticles**

Anthony D'Aléo,^{*[a]} Abdellah Felouat,^[a] Vasile Heresanu,^[a] Alain Ranguis,^[a] Damien
Chaudanson,^[a] Artak Karapetyan,^[a,b] Michel Giorgi,^[c] Frédéric Fages^[a]

[a] Aix Marseille Université, CNRS, CINaM UMR 7325, 13288 Marseille, France. [b] NAS
Armenia, Inst Phys Res, Ashtarak 2, Armenia. [c] Aix Marseille Université, CNRS,
Spectropole FR 1739, 13397 Marseille, France.

E-mail : daleo@cinam.univ-mrs.fr

Supporting information

Table of contents

Experimental part.	p2
Figure S1. ^1H NMR spectrum of Lig 2	p6
Figure S2. ^{13}C NMR spectrum of Lig 2	p6
Figure S3. ^1H NMR spectrum of 2	p7
Figure S4. ^{13}C NMR spectrum of 2	p8
Figure S5. Comparison of the calculated powder X-ray diffraction pattern with the experimental one for 1 .	p8
Figure S6. Nanoparticle size distribution determined by DLS for a/ dye 1 and b/ dye 2 .	p9
Figure S7. TEM images of the particles of a/ dye 1 and b/ dye 2	p9
Figure S8. Lippert-Mataga slopes for dyes 1 (■, black) and 2 (▲, red) and their respective linear fits.	P10
Figure S9. Normalized spectra of UV/visible absorption (a) and fluorescence emission (b) in THF upon addition of water for 1 .	p10
Figure S10. Normalized spectra of UV/visible absorption (a) and fluorescence emission (b) in THF upon addition of water for 2 .	p10
Figure S11. Evolution of the Stokes shift of a THF solution of 1 (a) and 2 (b) upon addition of water.	p11
Figure S12. Photoluminescence lifetimes of the particles of dye 1 (■), dye 2 (■) and their fits (—).	p11
Figure S13. Dependencies of the fluorescence intensity versus laser excitation power for 1 in DCM (■, black) and particles of 1 in water (▲, red).	p11
Table S1. Selected crystal data for dye 1 .	p12
References	p12

Experimental part

Materials and Instrumentation.

Spectroscopy. Solid state spectra and luminescence quantum yield were measured using an integration sphere. Solution state luminescence quantum yields Φ_f were measured in diluted solution with an absorbance lower than 0.1 at the excitation wavelength using the following equation $\Phi_{fx}/\Phi_{fr} = [A_r(\lambda)/A_x(\lambda)][D_x/D_r]$ where A is the absorbance at the excitation wavelength (λ), n the refractive index and D the integrated luminescence intensity. Subscripts “r” and “x” stand for reference and sample, respectively. The luminescence quantum yields were not corrected by the refractive indices. We used ruthenium trisbipyridine bischloride in water ($\Phi_{fr} = 0.021$) as reference compound. The luminescence quantum yields were double-checked using chalcone boron difluoride compounds previously reported. Luminescence lifetimes were determined by a method adapted for time-correlated single-photon counting. For these measurements, pulsed LEDs with the appropriate wavelength were used. Emission was monitored perpendicular to the excitation pulse.

X-ray Crystallography. The intensity data for the single-crystal X-ray diffraction analysis of **M4** were collected at room temperature on diffractometer using MoK $_{\alpha}$ radiation ($\lambda=0.71073$ Å). Data collection was performed with COLLECT,¹ cell refinement and data reduction with DENZO/SCALEPACK.² The structure was solved with SIR92³ and SHELXL-97⁴ was used for full matrix least squares refinement. The H-atoms were then introduced at idealized positions and constraint to their parent atom during the last refinements. Graphics were generated with MERCURY 2.4.

AFM and TEM AFM samples were characterized using a commercial instrument Nanoscope III (Digital Instruments Metrology Group, model MMAFM) in tapping mode under atmosphere at room temperature and, using standard μ mash[®] SPM probe

(NSC15/AIBS) with tip height of 20-25 μ m, cone angle inferior to 40°, tip radius inferior to 10nm (Resonant frequency 325kHz, force constant of \sim 46N/m). The images (512x512 pixels) were recorded at a line frequency of 1.5 Hz (Figure 3d) and 2.5 Hz (Figure 3e). Image analysis was performed with free SPM data analysis software Gwyddion®. For transmission electron microscopy, a JEOL 200 KV 2010 with a resolution of 2.3Å equipped with an X-ray analysis system (Quantax from Bruker) was used.

General Experimental Methods.

All solvents for synthesis were of analytic grade. Spectroscopy measurements were carried out with spectroscopic grade solvents. NMR spectra (^1H , ^{13}C , ^{19}F) were recorded at room temperature on a BRUKER AC 250 operating at 250, 62.5, and 235 MHz for ^1H , ^{13}C , and ^{19}F , respectively. Data are listed in parts per million (ppm) and are reported relative to tetramethylsilane (^1H and ^{13}C); residual solvent peaks of the deuterated solvents were used as an internal standard. Mass spectra and elemental analyses were realized in Spectropole de Marseille (<http://www.spectropole.fr/>).

Synthesis.

(1E,4Z,6E)-5-hydroxy-1,7-bis(2-methoxynaphthalen-1-yl)hepta-1,4,6-trien-3-one (Lig 2)

In a 100 mL round bottom flask, the acetylacetone (1.01g, 10.0mmol) and B_2O_3 (348mg, 0.5 mol eq) were mixed in 25 mL of ethyl acetate and stirred at 60 °C for 30 min. A solution of 2-methoxy-1-naphthaldehyde (3.72g, 20.0mmol) and n-tributylborane (4.60g, 20.0mmol) in 10 mL of ethyl acetate was added and the mixture was stirred for 30 min at 60 °C. A catalytic amount of butylamine (293, 4mmol) was then added to the

solution and the reaction mixture was refluxed overnight. After cooling to 50 °C, 30 mL of 0.4 M HCl was added to the mixture and stirred for 30 min at this temperature. After cooling, the precipitate was filtered off, washed with cold ethanol (30mL), diethyl ether (50mL) and pentane (50mL) and dried *in vacuo* to yield pure ligand **2**. Orange solid, yield: 61% (m= 2.66g)

¹H-NMR (CDCl₃, 250MHz): 8.37 (d, ³J= 16.0Hz, 2H), 8.27 (d, ³J= 8.5Hz, 2H), 7.86 (d, ³J= 9.0Hz, 2H), 8.80 (d, ³J= 7.5Hz, 2H), 7.54 (dt, ³J= 8.5Hz, ⁴J= 1.5Hz, 2H), 7.39 (dt, ³J= 8.0Hz, ⁴J= 1.0Hz, 2H), 7.31 (d, ³J= 9.2Hz, 2H), 6.92 (d, ³J= 15.8Hz, 2H), 5.94 (s, 1H), 4.04 (s, 6H); ¹³C-NMR (CDCl₃, 62.5MHz): 184.05, 156.79, 133.54, 132.87, 131.43, 129.44, 129.09, 128.60, 127.37, 123.92, 123.52, 117.56, 112.86, 102.29, 56.29. HRMS (ESI+) [M + Na]⁺ calcd for C₂₉H₂₅O₄⁺ 437.1747, found 437.1749.

(1E,4Z,6E)-5-(difluoroboryloxy)-1,7-bis(2-methoxynaphthalen-1-yl)hepta-1,4,6-trien-3-one (2)

In a 50 mL round bottom flask, the ligand (210mg, 0.481mmol) was solubilized in dichloromethane (20 mL) and boron trifluoride etherate (89mg, 0.620mmol) was added to this solution. The reaction mixture was refluxed overnight. After cooling to room temperature, the solvent was evaporated and the resulting solid was suspended into diethyl ether. The precipitate was filtered off and the black powder was washed with diethyl ether (40mL) and pentane (50mL) yielding the pure borondifluoride complex. Black solid, yield: 96% (m= 224mg).

¹H-NMR (DMSO-*d*₆, 250MHz): 8.67 (d, ³J= 15.8Hz, 2H), 8.30 (d, ³J= 8.5Hz, 2H), 8.17 (d, ³J= 9.2Hz, 2H), 7.98 (d, ³J= 7.5Hz, 2H), 7.68 (dt, ³J= 8.3Hz, ⁴J= 1.3Hz, 2H), 7.60 (d, ³J= 9.2Hz, 2H), 7.49 (t, ³J= 7.5Hz, 2H), 7.42 (d, ³J= 15.8Hz, 2H), 7.00 (s, 1H), 4.12 (s, 6H); ¹⁹F-NMR (CDCl₃, 235MHz): -140.65 (¹⁰B, 0.2F), -140.72 (¹¹B, 0.8F); ¹³C-NMR (CDCl₃, 62.5MHz): 180.45, 158.77, 139.51, 133.78, 133.25, 128.97, 128.84, 128.21, 125.19,

124.39, 123.13, 116.35, 112.52, 102.89, 56.26. HRMS (ESI+) $[M + Na]^+$ calcd for $C_{29}H_{23}O_4F_2BNa^+$ 507.1555, found 507.1533.

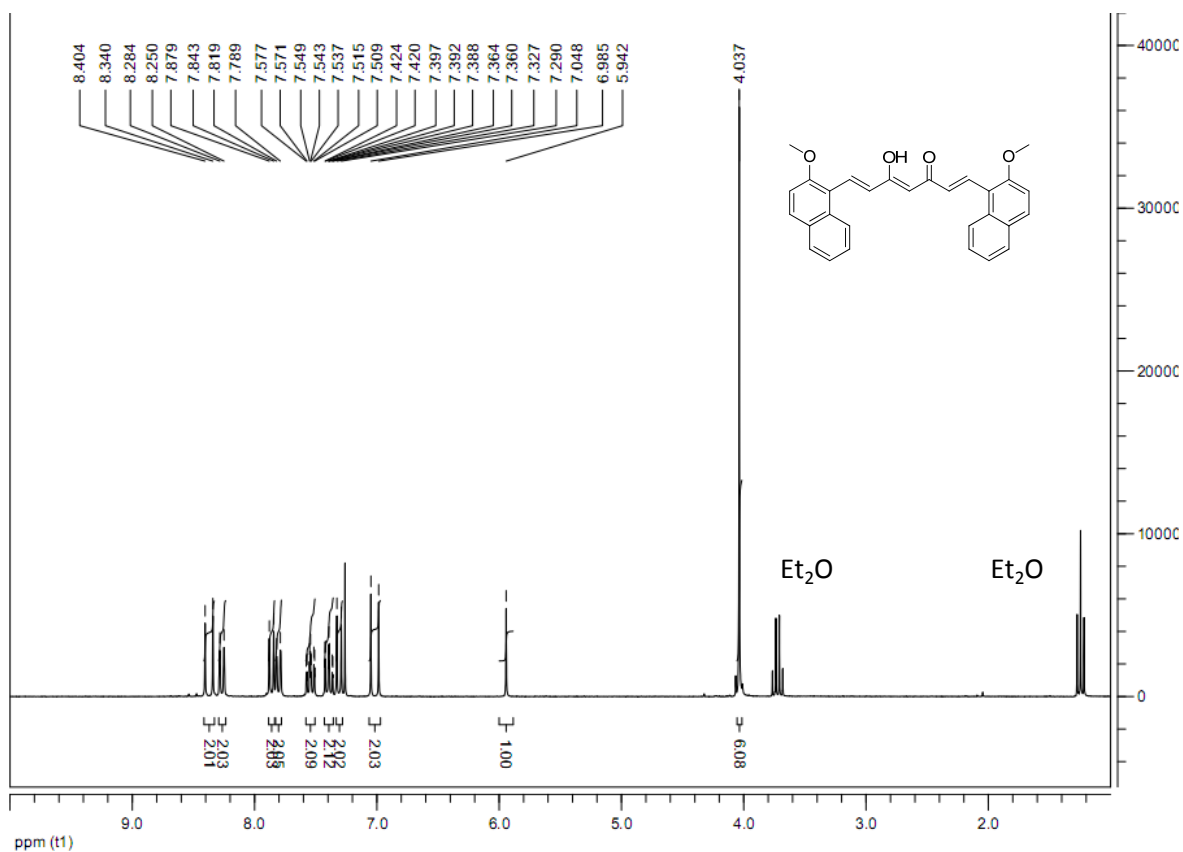


Figure S1. ^1H NMR spectrum of **Lig 2** ((1E,4Z,6E)-5-hydroxy-1,7-bis(2-methoxynaphthalen-1-yl)hepta-1,4,6-trien-3-one) in CDCl_3

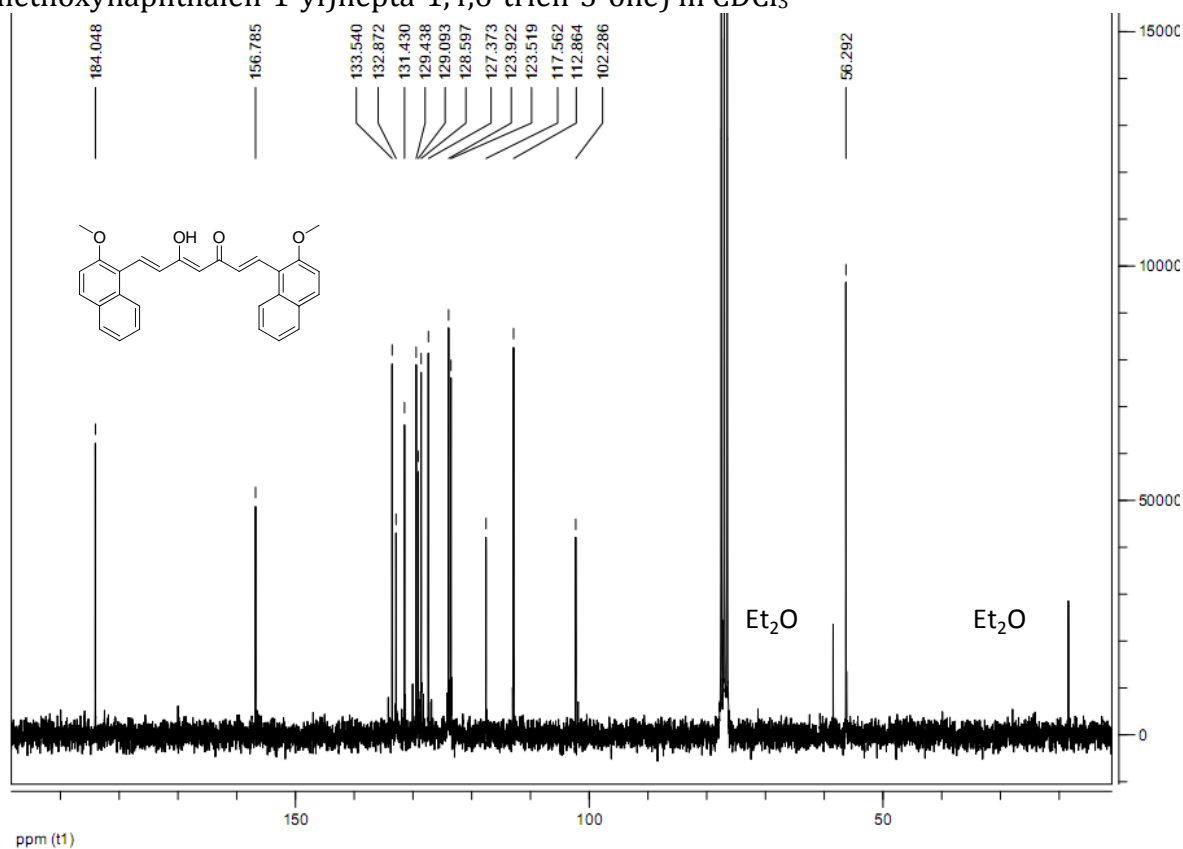


Figure S2. ^{13}C NMR spectrum of **Lig 2** ((1E,4Z,6E)-5-hydroxy-1,7-bis(2-methoxynaphthalen-1-yl)hepta-1,4,6-trien-3-one) in CDCl_3

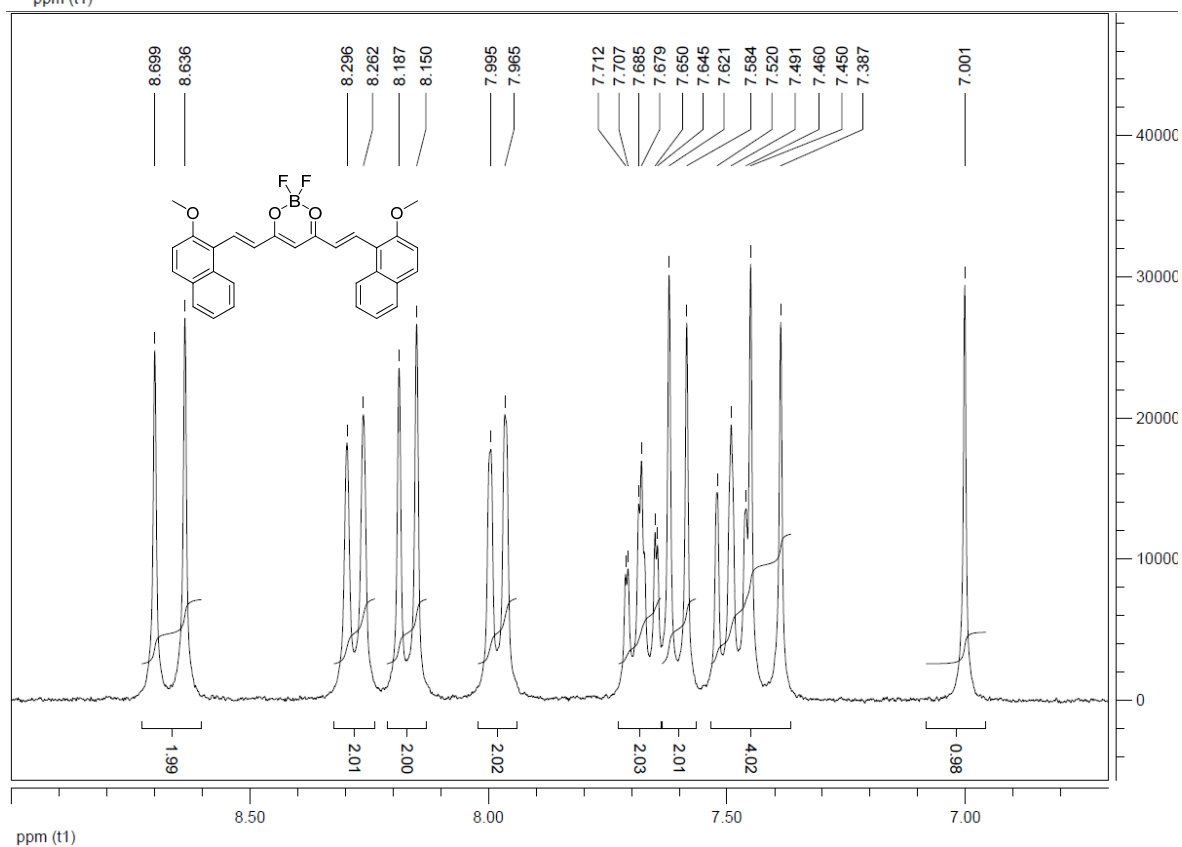
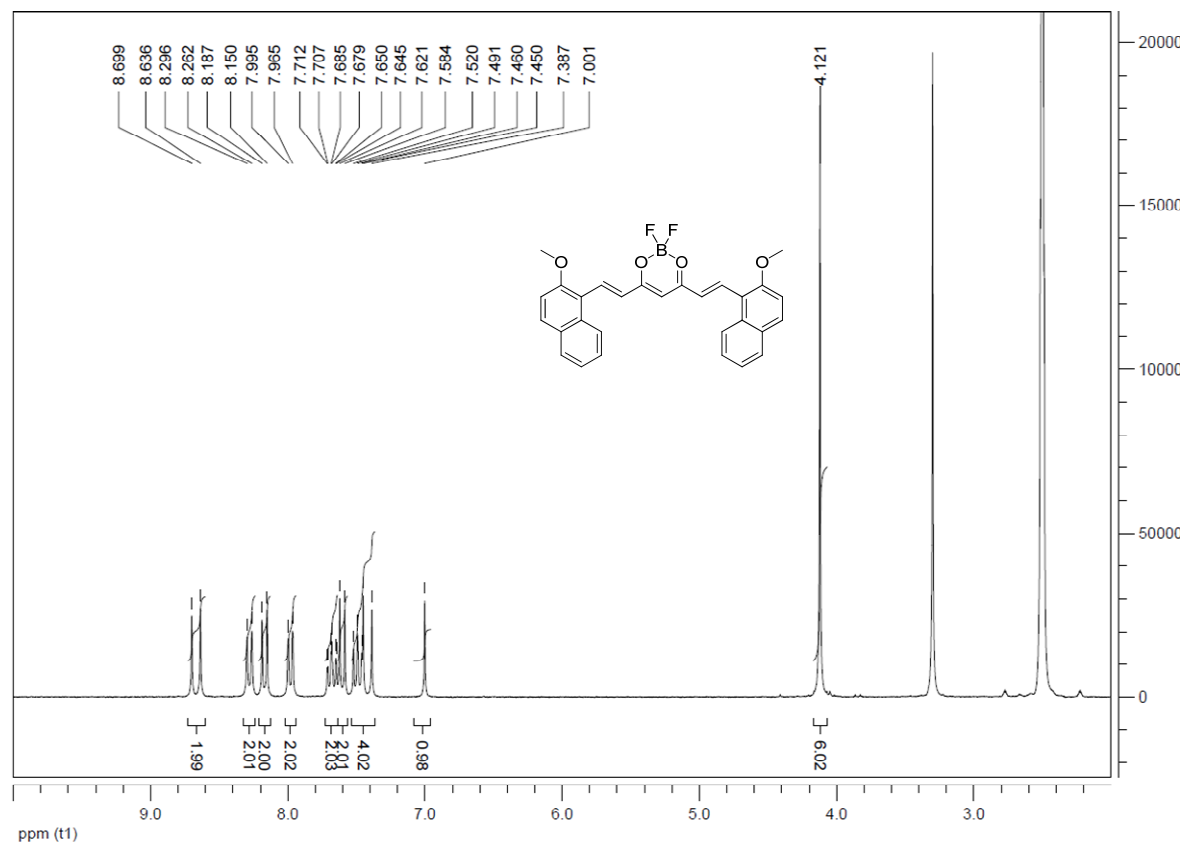


Figure S3. ^1H NMR spectrum of **2** ((1E,4Z,6E)-5-(difluoroboryloxy)-1,7-bis(2-methoxynaphthalen-1-yl)hepta-1,4,6-trien-3-one) in DMSO-d_6 (top: full spectrum, down: aromatic part)

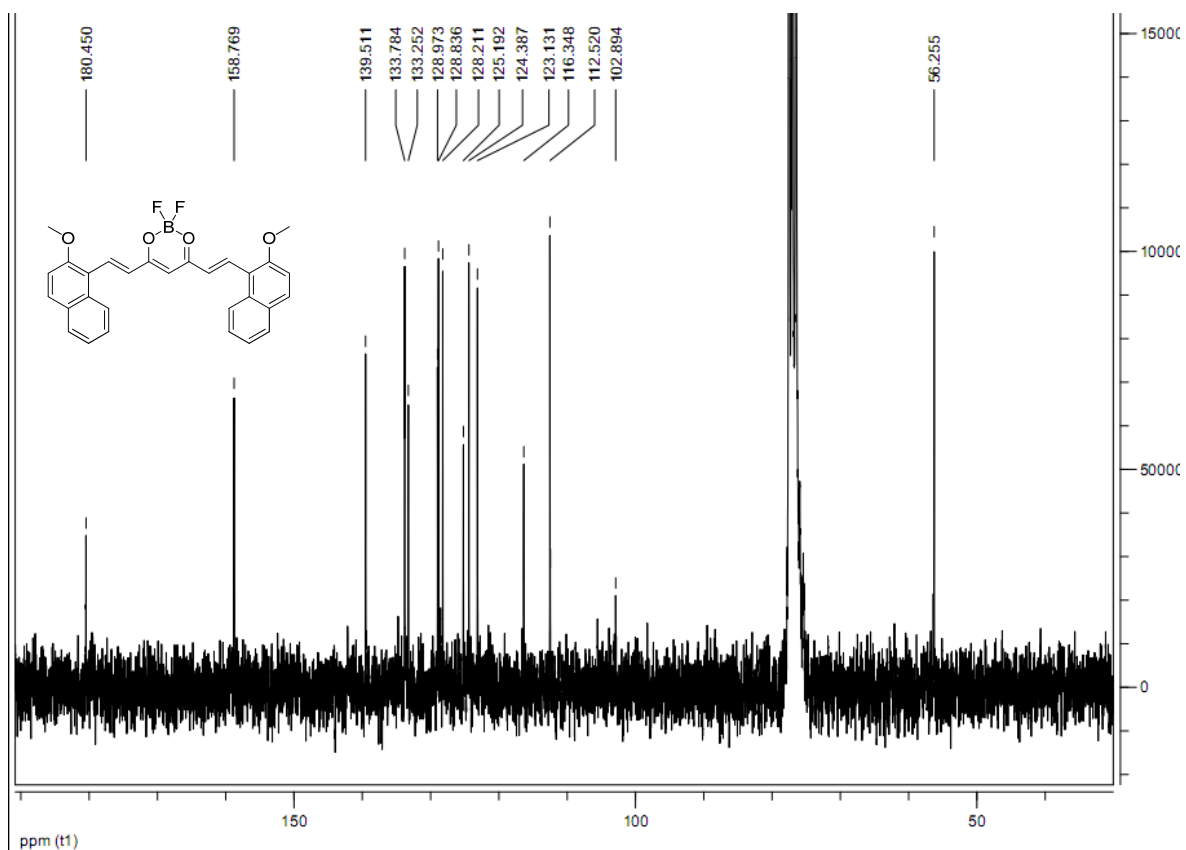


Figure S4. ^{13}C NMR spectrum of **2** ((1E,4Z,6E)-5-(difluoroboryloxy)-1,7-bis(2-methoxynaphthalen-1-yl)hepta-1,4,6-trien-3-one) in CDCl_3

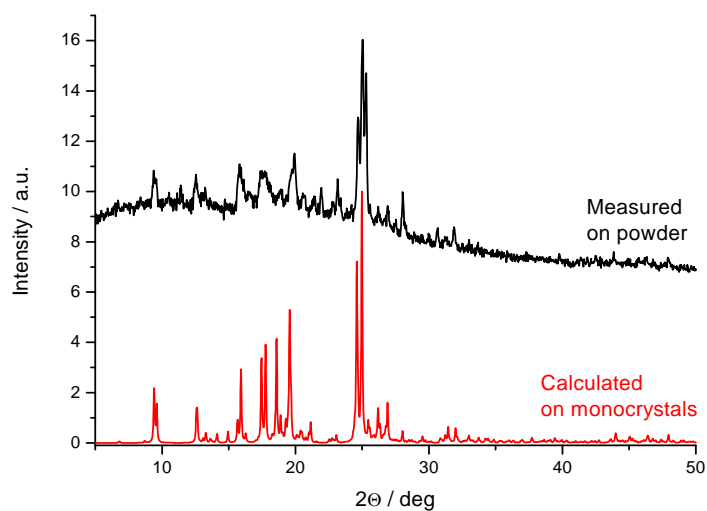


Figure S5. Comparison of the calculated powder X-ray diffraction pattern with the experimental one for **1**.

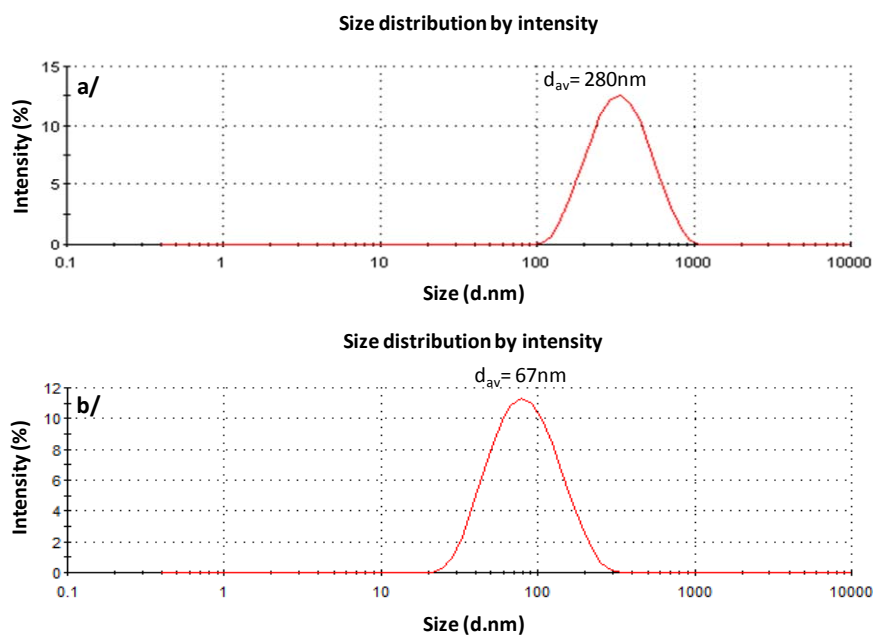


Figure S6. Nanoparticle size distribution determined by dynamic light scattering for a/ dye 1 ($[1] = 6.5 \times 10^{-6}\text{M}$, PDI= 0.410) and b/ dye 2 ($[2] = 4.4 \times 10^{-6}\text{M}$, PDI= 0.433).

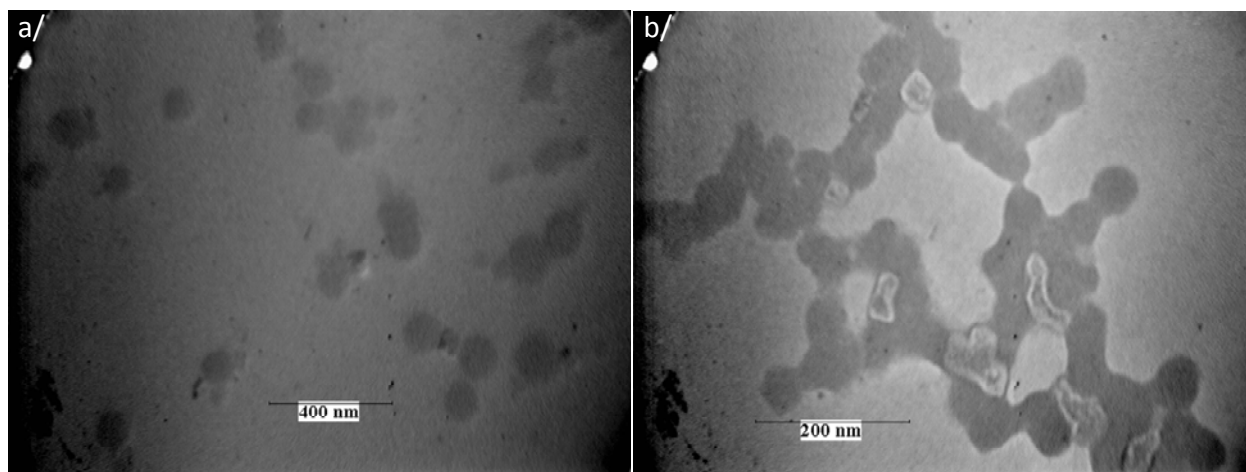


Figure S7. TEM images of the particles of a/ dye 1 and b/ dye 2.

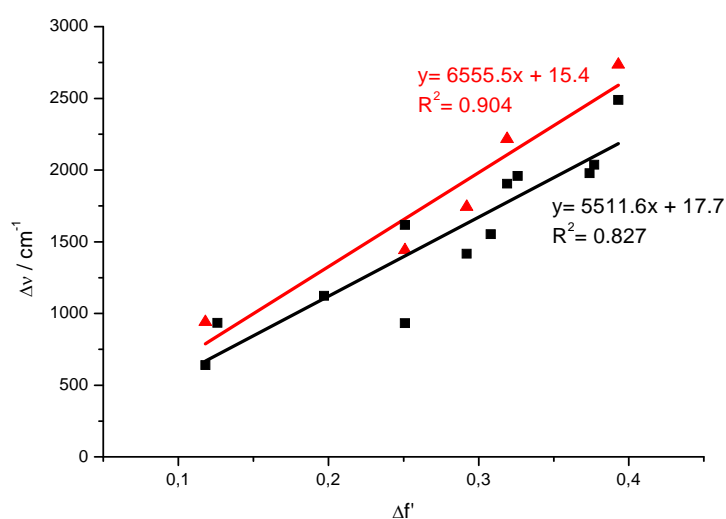


Figure S8. Lippert-Mataga plots for dyes **1** (■, black) and **2** (▲, red) and their respective linear fits.

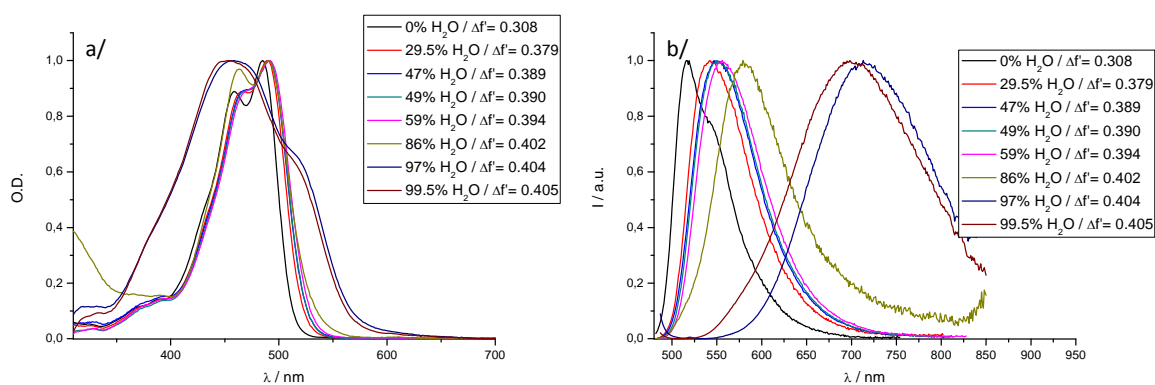


Figure S9. Normalized spectra of UV/visible absorption (a) and fluorescence emission (b) in THF upon addition of water for **1**.

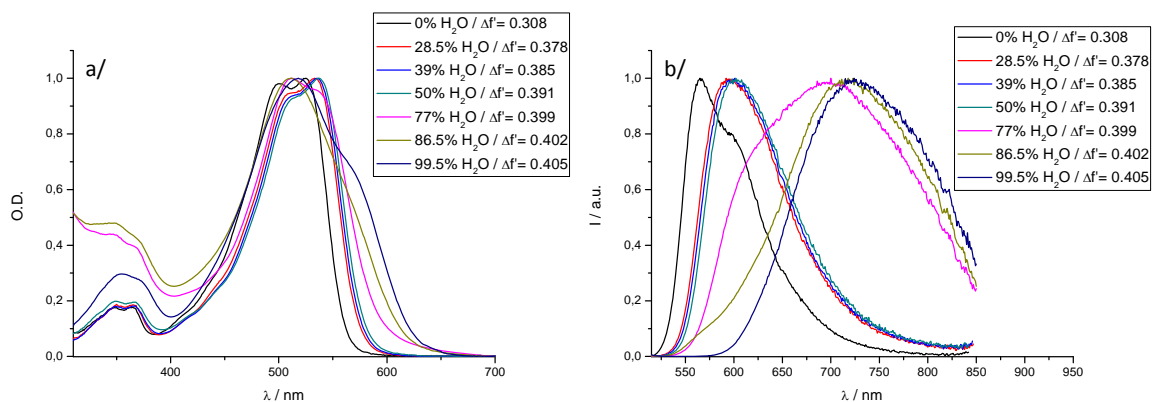


Figure S10. Normalized spectra of UV/visible absorption (a) and fluorescence emission (b) in THF upon addition of water for **2**.

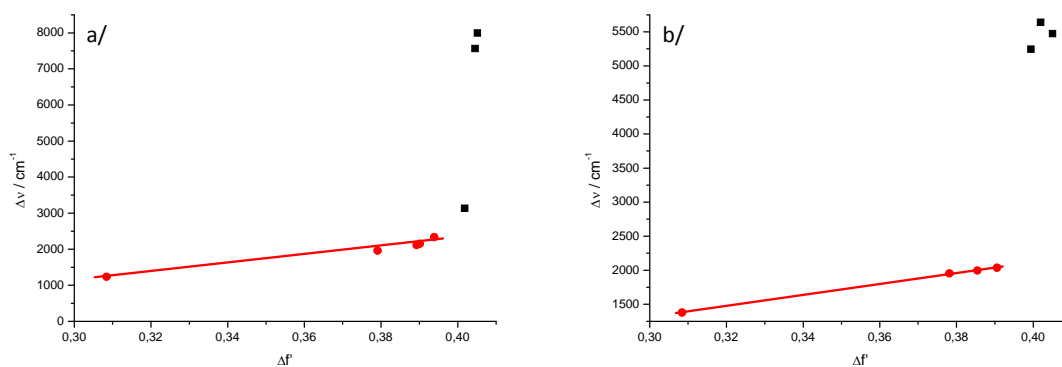


Figure S11. Evolution of the Stokes shift of a THF solution of **1** (a) and **2** (b) upon addition of water.

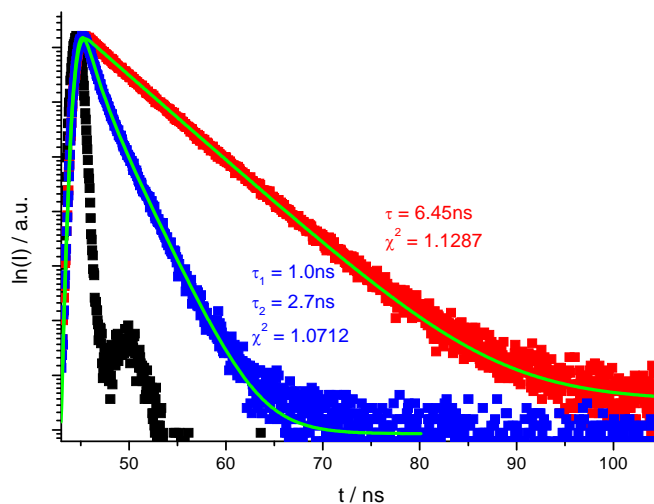


Figure S12. Photoluminescence lifetimes of the particles of dye **1** (■), dye **2** (■) and their fits (—); ■ represents the prompt.

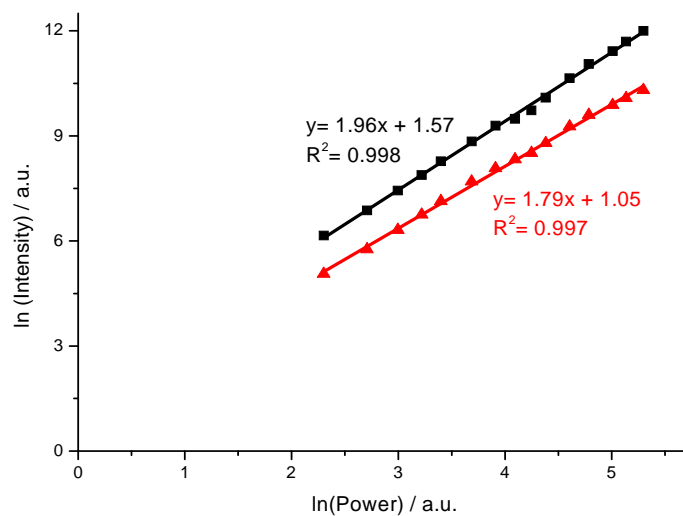


Figure S13. Dependencies of the fluorescence intensity versus laser excitation power for **1** in DCM (■, black) and particles of **1** in water (▲, red).

Table S1. Selected crystal data for dye 1.

Dye 1			
Formula	C ₂₄ H ₁₉ BF ₂ O ₄	$\lambda(\text{Mo}/K\alpha) / \text{\AA}$	0.71073
M / g	384.17	T / K	293(2)
Size / mm ³	0.30 x 0.18 x 0.06	Dc / g.cm ⁻³	1.333
Crystal System	Triclinic	θ range / deg	1.56 – 26.37
Space group	P ₋₁	<i>hkl</i> ranges	0, 13 -15, 17 -16, 17
<i>a</i> / \AA	11.1429(4)	Variable	505
<i>b</i> / \AA	14.0177(4)	Refln measured	7794
<i>c</i> / \AA	14.2677(5)	Refln $I > 2\sigma(I)$	3153
α / deg	73.452(1)	R1 $I > 2\sigma(I)$	0.0792
β / deg	68.556(1)	R1 all data	0.1912
γ / deg	69.722(1)	$wR2 I > 2\sigma(I)$	0.2264
<i>V</i> / \AA ³	1913.58(11)	$wR2$ all data	0.308
<i>Z</i>	2	$\Delta\rho (+/-) / e. \text{\AA}^{-3}$	0.256 / -0.338

References

1. Nonius BV: Delft, The Netherlands, 2001.
2. Otwinowski, Z.; Minor, W., Methods in Enzymology. In *Macromolecular Crystallography, Part A*, Carter Jr, C. W.; Sweet, R. M., Eds. Academic Press: New York, 1997; Vol. 276, pp 307–326.
3. Altomare, A.; Cascarano, G.; Giacovazzo, G.; Guagliardi, A.; Burla, M. C.; Polidori, G.; Camalli, M., *J. Appl. Cryst.* **1994**, 27, 435 – 435.
4. Sheldrick, G. M., *Acta Crystallogr. A* **2008**, 64, 112-122.